Enhancement of Higgs Production Through Leptoquarks at the LHC

by

Arvind Bhaskar, Debottam Das, Bibhabasu De, Subhadip Mitra

in

arXiv preprint arXiv:2002.12571

Report No: IIIT/TR/2020/-1

Centre for Computational Natural Sciences and Bioinformatics
International Institute of Information Technology
Hyderabad - 500 032, INDIA
February 2020

Enhancement of Higgs Production Through Leptoquarks at the LHC

IP-BBSR/2020-2

Arvind Bhaskar,[1,*] Debottam Das,[2,3,†] Bibhabasu De,[2,3,‡] and Subhadip Mitra[1,§]

[1]*Center for Computational Natural Sciences and Bioinformatics, International Institute of Information Technology, Hyderabad 500 032, India*

[2]*Institute of Physics, Sachivalaya Marg, Bhubaneswar 751 005, India*

[3]*Homi Bhabha National Institute, Training School Complex, Anushakti Nagar, Mumbai 400 085, India*

(Dated: March 2, 2020)

The Standard Model (SM) when extended with a Leptoquark (LQ) and right handed neutrinos, can have interesting new implications for Higgs physics. We show that the sterile neutrinos can induce a significant boost to the down-type quark Yukawa interactions through a diagonal coupling associated with the quarks and a scalar LQ of electromagnetic charge $1/3$. The relative change is much more pronounced in case of the first two generations of quarks as they have vanishingly small Yukawa couplings in the SM. The enhancement in the couplings would also lead to a non-negligible contribution of the quark fusion process to the production of the 125 GeV Higgs scalar in the SM, though the gluon fusion always dominates. However, this may not be true for a general scalar. As an example, we consider a scenario with a SM-gauge-singlet scalar ϕ where an $\mathcal{O}(1)$ coupling between ϕ and the LQ is allowed. The $\phi q\bar{q}$ Yukawa couplings can only be generated radiatively through a loop of LQ and sterile neutrinos. Here, the quark fusion process can have significant cross section, specially for a light ϕ. It can even supersede the normally dominant gluon fusion process for a moderate to large value of the LQ mass. This model can be tested/constrained at the high luminosity run of the LHC through a potentially large branching fraction of the scalar to two-jets.

I. INTRODUCTION

The discovery of a Standard Model (SM) like Higgs boson of mass 125 GeV at the LHC [1, 2] and the subsequent measurements of its couplings to other SM particles have played a significant role in understanding the possible physics beyond the Standard Model (BSM). The Higgs couplings to the third generation fermions and the vector bosons have already been measured within 10%-20% of their SM predictions [3]. However, it is difficult to put strong bounds on the Yukawa couplings (y_f) of the first two generations of fermions. For example, the present upper limits on y_μ and y_e are about 1.5 and 600 times their predicted values, respectively [3, 4]. Similarly, the light-quark Yukawa couplings are not yet measured directly. One can put much weaker bounds on them from a global fit to the available Higgs data [5, 6]. An analysis of Higgs boson pair production suggests that in future, the High Luminosity LHC (HL-LHC) may offer a better handle in this measurement [7]. An updated analysis, with 3000 fb^{-1} of integrated luminosity suggests (though not in a fully model independent way) that it may be possible to narrow down the d- and s-quark Yukawa couplings to about 260 and 13 times to their SM values, respectively [8], i.e.,

$$|\kappa_d| \leq 260, \qquad |\kappa_s| \leq 13, \tag{1}$$

where we have defined the Yukawa coupling modifiers κ_q as,

$$\kappa_q = \frac{y_q^{\rm eff}}{y_q^{\rm SM}}. \tag{2}$$

This gap between the reach of the LHC and the SM values of the light quark Yukawas suggests some scope for new physics to play. It is then interesting to investigate how one can enhance the Yukawa couplings of the light quarks without violating the tighter bounds on the third generation fermions and vector bosons. Recently, there have been some attempts on a possible universal enhancement of the Yukawa couplings of the light quarks that can be observed [9, 10]. In this paper, we try to motivate a simple extension to the SM augmented with a scalar Leptoquark (LQ) of electromagnetic charge $1/3$ (generally denoted as S_1) and right handed neutrinos that can effectively enhance the Yukawa couplings of the down-type quarks.

LQs are bosons that couple simultaneously to a quark and a lepton. They appear quite naturally in several extensions of the SM, specially in the theories of grand unification like Pati-Salam model [11], $SU(5)$ [12] or $SO(10)$ [13] (for a review see [14]). Though, in principle, LQs can either be scalar or vector in local quantum field theories, the scalar states are more attractive as the vector ones may lead to some problems with loops [15, 16]. In recent times, LQ models (with or without right handed neutrinos) have drawn attention for various reasons. For example, they can be used to explain different B-meson anomalies [17–24] or to enhance flavor violating decays of Higgs and leptons like $\tau \to \mu\gamma$ and $h \to \tau\mu$ [25]. LQs may also play a role to accommodate dark matter abundance [26, 27] or to mitigate the discrepancy in the anomalous magnetic moment of muon $(g-2)_\mu$ [28–30]. Direct production of TeV scale right handed neutrinos at the LHC can be strongly enhanced if one considers that the neutrino mass is generated at the tree level via the Inverse-Seesaw mechanism within LQ scenarios [31]. The collider phenomenology of various LQs have also been extensively discussed in the literature [14, 32–39].

In the scenario we consider, there are three generations of right chiral neutrinos in addition to the S_1. Generically, such a scenario is not very difficult to realize within the grand unified frameworks. In particular considering sterile neutrinos in this context, is not unusual. In fact, such a consideration is well motivated from the existence of nonzero neutrino masses and mixings which have been firmly established by now. It is known that an $\mathcal{O}(1)$ Yukawa coupling between the chiral neutrinos and TeV scale masses for the right handed neutrinos

* arvind.bhaskar@research.iiit.ac.in
† debottam@iopb.res.in
‡ bibhabasu.d@iopb.res.in
§ subhadip.mitra@iiit.ac.in

can explain the experimental observations related to neutrino masses and mixing angles even at the tree level if one extends SM to a simple set-up like the Inverse Seesaw mechanism [40–42] (ISSM). Of course, this requires the presence of an additional singlet neutrino state, X in the model [1].

Interestingly, the production cross sections of sterile neutrinos at the LHC can be enhanced significantly if the ISSM is embedded in a LQ scenario [31]. Similarly, a ν_R state in a loop accompanied with an S_1 may influence the production of the SM-like Higgs at the LHC and its decays to the SM fermions, especially to the light ones. Observable effects can be seen in scenarios with a general scalar sector (that may include additional Higgs states), a TeV scale ν_R and an $\mathscr{O}(1)$ Yukawa couplings between the left and right chiral neutrinos. In this paper we shall explore this in some detail. Notably, the gluon fusion process (ggF) for producing a Higgs scalar gets boosted in presence of a LQ [50]. Our study is general, can be applied to both the SM-like and BSM Higgs bosons. Specifically, we consider two cases:

A 125 GeV SM-like Higgs boson (h_{125}): We mainly investigate how the light-quark Yukawa couplings can get some positive boosts. As we shall see, the boosts can be significantly larger than the vanishing tree level values leading to enhancement of both production and decays of h_{125} at the LHC. These can be probed in the future LHC searches. Note that, in general, such large radiative corrections may induce corrections to the masses of the light quarks. Hence, some fine-tuning of the bare Lagrangian parameters may be required to produce the correct physical masses of the light quarks [7].

A singlet scalar ϕ (BSM Higgs): We also study the productions and decays of a scalar ϕ that is a singlet under the SM gauge group. Such a scalar has been considered in different contexts in the literature earlier. For example, it may serve as a dark matter candidate. Similarly, a singlet scalar can help solve the so called μ problem in the Minimal Supersymmetric Standard Model [51]. To produce such a singlet at the LHC, one generally relies upon its mixing with the doublet like Higgs states present in the theory. If the mixing is non-negligible, then the leading order production process turns out to be the gluon fusion (though vector boson fusion (VBF) may also become relevant in specific cases [52]). One may also consider the production of ϕ through cascade decays of the doublet Higgs state(s). However, such a process is generally much suppressed. Now, as we shall see, in the presence of a scalar LQ and sterile neutrinos we could have a new loop contribution to the quark fusion production process (qqF). The LQ would also contribute to the gluon fusion process. In such a set-up, the singlet Higgs can potentially be tested at the LHC via its decays to the light quark states.

The rest of the paper is organised as follows. In section II we introduce the model Lagrangian and discuss the new interactions. In section III, we discuss the additional contributions to the production and decays of h_{125}. In section IV, we discuss the bounds on the parameters. In section V, we investigate the case of the singlet scalar ϕ. Finally we summarize our results and conclude in section VI.

[1] ISSM or Inverse Seesaw extended supersymmetric models may lead to interesting phenomenology at the low energy [43–49]

II. THE MODEL: A SIMPLE EXTENSION OF THE SM

As explained in the introduction, our model is a simple extension of the SM with chiral neutrinos and an additional scalar LQ of electromagnetic charge $1/3$, normally denoted as S_1. The LQ transforms under the SM gauge group as $(\bar{\mathbf{3}},\mathbf{1},1/3)$ with $Q_{\rm EM}=T_3+Y$. In the notation of Ref. [14], the general fermionic interaction Lagrangian for S_1 can be written as,

$$\mathscr{L}_F = (y_1^{LL})_{ij}(\bar{Q}_L^{Cia}\varepsilon^{ab}L_L^{jb})S_1+(y_1^{RR})_{ij}(\bar{u}_R^{Ci}e_R^j)S_1 + (y_1^{\overline{RR}})_{ij}(\bar{d}_R^{Ci}\nu_R^j)S_1+\text{H.c.}, \tag{3}$$

where we have suppressed the color indices. The superscript C denotes charge conjugation; $\{i,j\}$ and $\{a,b\}$ are flavor and $SU(2)$ indices, respectively. The SM quark and lepton doublets are denoted by Q_L and L_L, respectively. We now add the scalar interaction terms to the Lagrangian in Eq. (3),

$$\mathscr{L} \supset \mathscr{L}_F + \lambda\left(H^\dagger H\right)\left(S_1^\dagger S_1\right)+\lambda'\phi\left(S_1^\dagger S_1\right) + \mu(H^\dagger H)\phi^2+\frac{1}{2}M_\phi^2\phi^2+\bar{M}_{S_1}^2\left(S_1^\dagger S_1\right). \tag{4}$$

Here, H denotes the SM Higgs doublet, M_ϕ and $\bar{M}_{S_1}$ define the bare mass parameters for ϕ and S_1, respectively. We denote the physical Higgs field after the electroweak symmetry breaking as $h\equiv h_{125}$. The singlet ϕ does not acquire any vacuum expectation value (VEV). Physical masses can be obtained via

$$H=\frac{1}{\sqrt{2}}\begin{pmatrix}0\\ v+h\end{pmatrix},\qquad \phi=\phi, \tag{5}$$

where the SM Higgs VEV, $v\simeq 246$ GeV. We assume the mixing between H and ϕ, controlled by the dimensionless coupling μ to be small to ensure that the presence of a singlet Higgs doesn't affect the production and decays of h_{125} significantly via mixing. Notice that unlike dimensionless λor μ, λ' is a dimension one parameter. We define the physical mass of S_1 to be M_{S_1} as:

$$M_{S_1}^2 \;=\; \bar{M}_{S_1}^2+\frac{1}{2}\lambda v^2\,. \tag{6}$$

The above Lagrangian simplifies a bit if we ignore the mixing among quarks and neutrinos (i.e., set $\mathbf{V}_{\rm CKM}=\mathbf{U}_{\rm PMNS}=\mathbb{I}$). For example, we can expand Eq. (4) for the first generation as,

$$\begin{aligned}\mathscr{L} \supset{}& \Big\{y_1^{LL}\left(-\bar{d}_L^C\nu_L+\bar{u}_L^Ce_L\right)S_1+y_1^{RR}\,\bar{u}_R^Ce_RS_1 \\ &+y_1^{\overline{RR}}\,\bar{d}_R^C\nu_RS_1+h.c.\Big\}+\lambda vh\left(S_1^\dagger S_1\right) \\ &+\lambda'\phi\left(S_1^\dagger S_1\right)+\frac{1}{2}M_\phi^2\phi^2+M_{S_1}^2\left(S_1^\dagger S_1\right),\end{aligned} \tag{7}$$

where we have simplified $\left(y_1^X\right)_{ii}$ as y_i^X. Since the flavor of neutrino is irrelevant for the LHC, here onward we shall simply write ν to denote neutrinos.

The terms in Eq. (7) have the potential to boost up some production/decay modes for h and ϕ. For example, it would lead to an additional contribution to the effective hgg coupling [see Fig. 1(a), 1(b)] [50]. Similarly, the decay $h\to d\bar{d}$, which is negligible in the SM, would get a boost now, as long as some of the new couplings are not negligible. The processes are illustrated in Figs. 1(c) and 1(d) where the Higgs is shown to

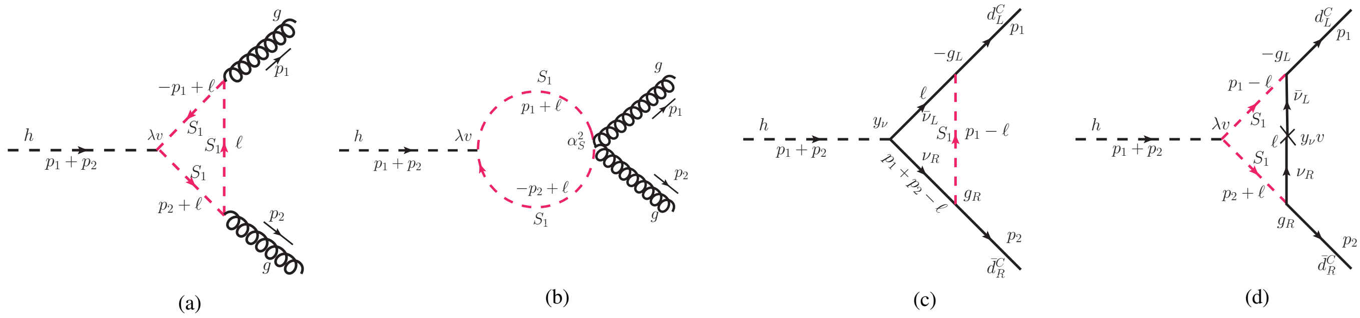

FIG. 1. Feynman diagrams showing the SM-like Higgs (h_{125}) decaying to gluon pairs [(a) and (b)] and down quarks [(c) and (d)] through loop diagrams mediated by S_1 and chiral neutrinos. Only in diagram (c) the Higgs couples to ν whereas in all the other diagrams, it couples to S_1. The couplings $g_L = y_1^{LL}$ and $g_R = y_1^{\overline{RR}}$ [see Eq. (7)]. The diagrams for s- and b-quarks are similar to the last two diagrams. Note that we absorb a factor of $1/\sqrt{2}$ in the definition of Yukawa couplings in the mass basis, i.e., we write y_ν instead of $y_\nu/\sqrt{2}$.

be decaying to a $d\bar{d}$ pair via a triangle loop mediated by S_1 and chiral neutrinos. There are two possibilities: either the Higgs directly couples with the chiral neutrinos or the LQ. Since the contributions of these diagrams appear as corrections to $\langle y_d\rangle$, it is easy to see that the fermion in the loop (i.e., the neutrino) has to go through a chirality flip. In this case, the right-handed neutrino from the third term in Eq. (3) helps in gettting a non-zero contribution.

One can, of course, imagine similar diagrams with charged leptons in the loops, contributing to the $h \to u\bar{u}$ (or any other up-type quark-anti-quark pair) decay. However, the contributions of such diagrams would be small as they are suppressed by the tiny charged lepton Yukawa couplings, at least for the first two generations. If we restrict ourselves only to flavour diagonal couplings in Eq. (3) (i.e., allow only $i = j$ terms), only the top Yukawa, y_t would be modified appreciably. If we allow off-diagonal couplings, one can get contributions for the first two generations Yukawa couplings, namely y_u or y_c respectively. However, one needs to be careful as off-diagonal LQ-quark-lepton couplings are constrained, particularly for the first two generations [14, 53]. In the present case, we consider only flavour diagonal couplings and look only at the modification of Higgs couplings to down type quarks. Thus one may always set $\left(y_1^{RR}\right)_{ij} = 0$ for all values of i and j. This may lead to a somewhat favourable situation in some cases to accommodate rare decays of fermions through LQ exchange.

Before we discuss productions and decays of h_{125} and ϕ in our model, a few comments are in order. As we shall see in the next section, an order one $h\bar{\nu}_L\nu_R$ coupling, i.e., $y_\nu \sim \mathcal{O}(1)$ and a TeV scale mass for the ν_R would be helpful to raise the Yukawa couplings of the light quarks. Typically, the models like ISSM would be able to accommodate such a scenario. In the ISSM, an additional gauge singlet neutrino, usually denoted by X, is assigned a Majorana mass term $\mu_X XX$ while ν_R receives a Dirac mass term of the form $M\bar{\nu}_R X$. For our purpose we may assume that this singlet X cannot directly interact with any other particle we consider. However, since it interacts exclusively with the ν_R fields via M, it would modify the ν_R propagators. In this case, it may be useful to define something called a “fat ν_R propagator” [54] that includes all the effects of the sequential insertions of the X field. We do not display this interaction and mass term of the right handed neutrinos explicitly in Eq. (3) for simplicity. One can explicitly consider an ISSM in the backdrop of our analysis and easily accommodate fat ν_R propagators without any change in our results.

III. CONTRIBUTION TO THE PRODUCTION AND DECAYS OF h_{125}

In this section, we first look into the additional contributions to the Yukawa couplings of the down-type quarks with h_{125}. The relevant interactions can be read from Eq. (7). We shall then discuss the role of these loops in the production of h_{125} and its decays to the down type quarks. In this paper, we compute all the loop diagrams using dimensional regularization and Feynman parametrization and then match the results using the Passarino-Veltman (PV) integrals [55]. We evaluate the PV integrals with two publicly available packages, FeynCalc [56] and LoopTools [57].

A. Correction to Yukawa Couplings of the Down-type Quarks

In our calculation, we assume that left-handed neutrinos are massless while the right-handed ones are massive. Also, since we consider Higgs decays to down-type quarks only, we can safely ignore the quark masses ($m_q = 0$) and set $m_h^2 = (p_1 + p_2)^2 = 2p_1.p_2$ (see Fig. 1). The correction to y_d coming from the diagram shown in Fig. 1(c) is given by,

$$\tilde{y}_d^{(a)} = -ig_1^2 y_\nu \int \frac{d^4\ell}{(2\pi)^4}\left[\frac{P_R \not{\ell}\,(\not{p}_1 + \not{p}_2 - \not{\ell} + M_{\nu_R})P_R}{\ell^2\{(p_1+p_2-\ell)^2 - M_{\nu_R}^2\}} \times \frac{1}{\{(p_1-\ell)^2 - M_{S_1}^2\}}\right], \tag{8}$$

where $g_1^2 = g_L g_R = y_1^{LL} y_1^{\overline{RR}}$ and $P_{L/R}$ are the chirality projectors. From here onwards we shall suppress the generation index of the leptoquark couplings and simply write g_i^2 as g^2. After Feynman parametrization and dimensional regularization we get,

$$\tilde{y}_d^{(a)} = -\frac{g^2 y_\nu}{16\pi^2}\left[\int_0^1 dx \int_0^{1-x} dy \left(\frac{x m_h^2}{D_1}\right) - \int_0^1 dz \ln D_2 + \Delta_\varepsilon\right], \tag{9}$$

where,

$$D_1(x,y) = xym_h^2 + x(x-1)m_h^2 + xM_{\nu_R}^2 + yM_{S_1}^2, \tag{10}$$

M_{ν_R} (GeV)	M_{S_1} (GeV)	$y^{(a)}(g^2 y_\nu = 1)$	$y^{(b)}(g^2 y_\nu = 1, \lambda = 1)$
500	1000	-0.000057	0.000275
	1500	-0.000037	0.000139
1000	1000	-0.000025	0.000192
	1500	-0.000018	0.000108

TABLE I. Contributions of the two diagrams shown in Fig. 1 to the Yukawa couplings as obtained from Eq. (15) or Eq. (16) for some illustrative choices of the mass of the right-handed neutrino, M_{ν_R} and the leptoquark mass, M_{S_1}.

and

$$D_2(z) = zM_{S_1}^2 + (1-z)M_{\nu_R}^2. \tag{11}$$

The divergent piece, $\Delta_\varepsilon = \frac{2}{\varepsilon} - \gamma + \ln(4\pi) + \mathscr{O}(\varepsilon)$, is cancelled by a similar contribution from the diagrams that consider a bubble in the an external quark line given as,

$$\frac{g^2 y_\nu}{16\pi^2} \int_0^1 dz \left[\Delta_\varepsilon - \ln\left\{zM_{S_1}^2 + (1-z)M_{\nu_R}^2\right\}\right]. \tag{12}$$

Putting these two together we get,

$$y_d^{(a)} = -\frac{g^2 y_\nu}{16\pi^2}\left[\int_0^1 dx \int_0^{1-x} dy \left(\frac{x m_h^2}{D_1}\right)\right]. \tag{13}$$

Now, proceeding along the same line, we get the correction from the diagram in Fig. 1(d) as,

$$\begin{aligned} y_d^{(b)} &= i g^2 \lambda y_\nu v^2 \int \frac{d^4\ell}{(2\pi)^4}\left[\frac{1}{(\ell^2 - M_{\nu_R}^2)\{(\ell-p_1)^2 - M_{S_1}^2\}} \right. \\ &\qquad \left. \times \frac{1}{\{(\ell+p_2)^2 - M_{S_1}^2\}}\right] \\ &= \frac{g^2 \lambda y_\nu v^2}{16\pi^2}\int_0^1 dx \int_0^{1-x} dy \left(\frac{1}{D_0}\right), \end{aligned} \tag{14}$$

where $D_0(x,y) = M_{\nu_R}^2 + (x+y)(M_{S_1}^2 - M_{\nu_R}^2) - xy m_h^2$. Therefore the effective $hd\bar{d}$ coupling can be written as,

$$\begin{aligned} y_d^{\rm eff} &= y_d^{\rm SM} + \delta y \\ &= \frac{m_d}{v} + \frac{g^2 y_\nu}{16\pi^2}\left[\int_0^1 dx \int_0^{1-x} dy \left(\frac{\lambda v^2}{D_0} - \frac{x m_h^2}{D_1}\right)\right], \end{aligned} \tag{15}$$

where $\delta y = y_d^{(a)} + y_d^{(b)}$ is the total loop correction. Eq. (15) can also be written in terms of the PV integrals,

$$\begin{aligned} y_d^{\rm eff} = \frac{m_d}{v} + \frac{g^2 y_\nu}{16\pi^2}&\Big[B_0(0, M_{\nu_R}^2, M_{S_1}^2) - B_0(m_h^2, 0, M_{\nu_R}^2) \\ &- M_{S_1}^2 C_0(0, 0, m_h^2, 0, M_{S_1}^2, M_{\nu_R}^2) \\ &- \lambda v^2 C_0(0, 0, m_h^2, M_{S_1}^2, M_{\nu_R}^2, M_{S_1}^2)\Big], \end{aligned} \tag{16}$$

where C_0 and B_0 are the triangle and the bubble integrals, respectively. The expressions for the s- and b-quarks would be exactly the same as above with m_d and $g^2 = g_i^2$ suitably modified.

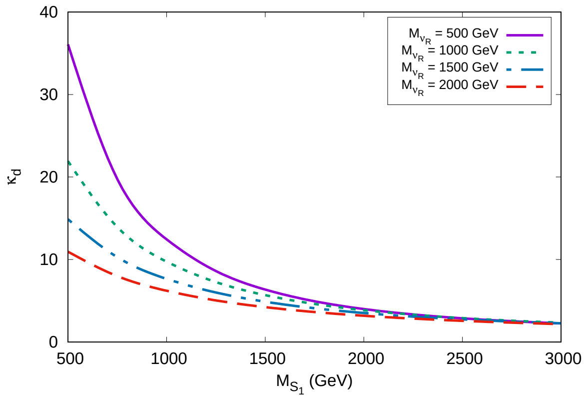

(a)

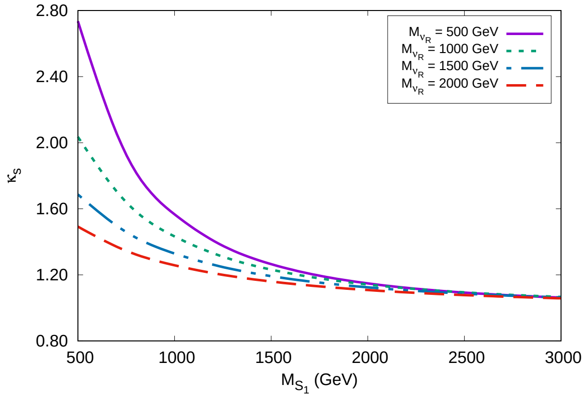

(b)

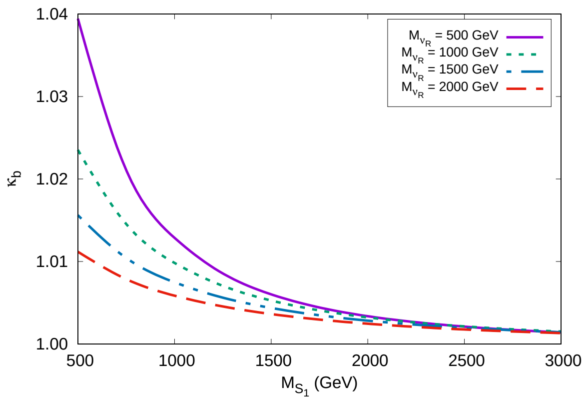

(c)

FIG. 2. Variation of the coupling modifiers κ_d (a), κ_s (b) and κ_b (c) [defined in Eq. (2)] with M_{S_1} for different values of M_{ν_R}. Here we set $g^2 y_\nu = 1$ for all the three generations and keep $\lambda = 1$.

B. Relative Couplings

To get some idea about how the extra contributions from the loops depend on the parameters, we first re-express Eq. (2) as,

$$\kappa_q = 1 + \frac{\delta y}{y_q^{\rm SM}}. \tag{17}$$

Since we ignore the mass of the quarks, δy is independent of the flavour of the down type quark that the Higgs is coupling

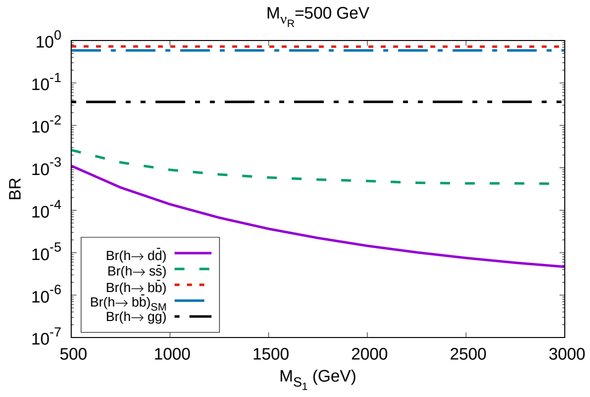

(a)

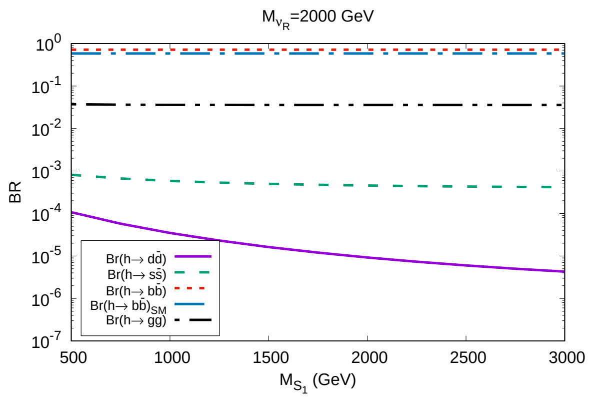

(b)

FIG. 3. Variation of $\mathrm{Br}(h \to ii)$ with M_{S_1} for $i = d, s, b$ and gluon. We have set $g^2 y_\nu = 1$ for all generations and taken $\lambda = 1$.

to as long as $g^2 y_\nu$ remains the same. Hence, $\delta y / y_q^{\rm SM}$ should go as $1/y_q^{\rm SM} \sim 1/m_q$. Using this and Eq. (16), we see that κ_q depends linearly on $1/m_q$, λ and the combination $g^2 y_\nu$ but, a priori, its dependence on M_{S_1} or M_{ν_R} is not so simple. In Table I, we show the contributions of the two loop diagrams (Fig. 1(c) and 1(d)) for some illustrative choices of M_{ν_R} and M_{S_1}. With $g^2 y_\nu = \lambda = 1$, we see that there is some cancellation between these contributions. Note that this choice of couplings is not restricted by the rare decays [14, 53]. For order one λ, $y^{(a)}$ is smaller than $y^{(b)}$, making $\delta y \propto \lambda g^2 y_\nu$.

In Fig. 2, we show the variations of κ_d, κ_s and κ_b for $500 \leq M_{S_1} \leq 3000$ GeV for four different choices of M_{ν_R}. As expected, we see the lightest among the three quarks, i.e., d-quark getting the maximum deviation in κ_q from unity. The b-quark coupling hardly moves from the SM value for the considered parameter range . However, all the limits are within the ranges allowed by Eq. (1).

C. Decays of h_{125}

As mentioned before, we shall use both h and h_{125} to denote the 125 GeV SM-like Higgs boson, interchangeably. In the SM, the total decay width of the 125 GeV Higgs boson is computed to be $\Gamma_h^{\rm SM} = 4.07 \times 10^{-3}$ GeV, with a relative theoretical uncertainty of ${}^{+4.0\%}_{-3.9\%}$ [58]. Now, because of the additional loop contribution, it would increase in our model. We can use Eq. (15) [or (16)] to compute the partial decay width for the $h \to q\bar{q}$ decay in the rest frame of the Higgs as,

$$\begin{aligned} \Gamma_{h\to q\bar{q}} &= N_c \times \frac{|\vec{p}_q|}{32\pi^2 m_h^2} \int |\mathscr{M}_{tot}|^2 \, d\Omega \\ &= \frac{N_c}{8\pi m_h^2} |y_q^{\rm eff}|^2 \left(m_h^2 - 4m_q^2\right)^{3/2}, \end{aligned} \tag{18}$$

where $i\mathscr{M}_{tot} = y_q^{\rm eff} q\bar{q}$ is the invariant amplitude and $N_c = 3$ accounts for the colours of the quark. Similarly, the $h \to gg$ partial width would also get a positive boost in presence of S_1 [14]. The relevant diagrams can be seen from Figs. 1(a) and 1(b). In our model, the $h \to gg$ partial width can be expressed as [14, 59],

$$\Gamma_{h\to gg} = \frac{G_{\rm F} \alpha_s^2 m_h^3}{64\sqrt{2}\pi^3} \left| \mathscr{A}_{1/2}(x_t) + \frac{\lambda v^2}{2M_{S_1}^2} \mathscr{A}_0(x_{S_1}) \right|^2 \tag{19}$$

where $x_t = m_h^2/4m_t^2$ and $x_{S_1} = m_h^2/4M_{S_1}^2$. The relevant one-loop functions are given by

$$\mathscr{A}_{1/2}(x) = \frac{2[x + (x-1)f(x)]}{x^2}, \tag{20}$$

$$\mathscr{A}_0(x) = -\frac{[x - f(x)]}{x^2}, \tag{21}$$

$$f(x) = \left\{ \begin{array}{ll} \arcsin^2(\sqrt{x}), & x \leq 1 \\ -\frac{1}{4}\left[\ln\left(\frac{1+\sqrt{1-x^{-1}}}{1-\sqrt{1-x^{-1}}}\right) - i\pi\right]^2, & x > 1 \end{array} \right\}. \tag{22}$$

Now, Eqs. (18) and (19) can be used to obtain the total width in our model,

$$\begin{aligned} \Gamma_h = &\left(\Gamma_h^{\rm SM} - \Gamma_{h\to gg}^{\rm SM} - \sum_{q=d,s,b} \Gamma_{h\to q\bar{q}}^{\rm SM\,(tree)} \right) + \Gamma_{h\to gg} \\ &+ \sum_{q=d,s,b} \Gamma_{h\to q\bar{q}}. \end{aligned} \tag{23}$$

Ideally, we should also include corrections to partial widths of other decay modes, like $h \to \gamma\gamma$ or other three body decays etc. in the above expression. However, since their contributions to the total width are relatively small, we ignore them.

From Eq. (18) and Eq. (23), we compute the new branching ratios (BRs) of the $h \to q\bar{q}$ modes in our model as,

$$\mathrm{Br}(h \to q\bar{q}) = \frac{\Gamma_{h\to q\bar{q}}}{\Gamma_h}. \tag{24}$$

In Fig. 3 we show $\mathrm{Br}(h \to q\bar{q})$ for different quarks for $g^2 y_\nu = 1$ (for all generations) and $\lambda = 1$. Eq. (18) indicates $\mathrm{Br}(h \to q\bar{q}) \sim |y_q^{\rm SM} + \delta y|^2$, i.e., it increases with $y_q^{\rm SM}$ (remember, for $g^2 y_\nu = 1$, δy is the same for all the quarks). Hence, we expect $\mathrm{Br}(h \to b\bar{b}) > \mathrm{Br}(h \to s\bar{s}) > \mathrm{Br}(h \to d\bar{d})$ as $y_q^{\rm SM}$ increases with the mass of the quark. This can be seen in Fig. 3. However, even for order one y_ν couplings and TeV scale S_1 and ν_R, the relative shift in branching ratio of the $h \to b\bar{b}$ decay to that of SM is not large (as expected from Fig. 2). For the lighter quarks, the branching ratios become much larger than their SM values, even though they remain small compared to other decay modes like $h \to b\bar{b}$. The branching fraction $h \to gg$ is almost unaffected with the variation in S_1 as the SM contribution always dominates.

D. Production of h_{125}

For a quantitative understanding of the quark-gluon fusion production of h_{125}, we normalise the fusion cross section with respect to its SM value. We define the “normalized production” factor $\mu_{\rm F}$ as,

$$\mu_{\rm F} \equiv \mu_{\rm F}^{gg+q\bar{q}} = \frac{\sigma(gg\to h)+\sum_{q=d,s,b}\sigma(q\bar{q}\to h)}{\sigma(gg\to h)_{\rm SM}}. \tag{25}$$

It is a function of the BSM parameters and measures the relative enhancement of production cross-section in the fusion channel. The subscript ‘F’ stands for the fusion channel. In the denominator we ignore $\sigma(b\bar{b}\to h)_{\rm SM}$ as it is much smaller than $\sigma(gg\to h)_{\rm SM}$ because of the small b-quark parton distribution function (PDF) in the initial states.

In our model, the leading order gluon fusion cross section at the parton level can be expressed as [14, 59–61],

$$\hat{\sigma}(gg\to h) = \frac{\pi^2 m_h}{8\hat{s}}\Gamma_{h\to gg}\,\delta(\hat{s}-m_h^2), \tag{26}$$

where $\Gamma_{h\to gg}$ is given in Eq. (19). Similarly, the quark fusion cross section at the parton level can be expressed in terms of $\Gamma_{h\to q\bar{q}}$ from Eq. (18) as [58],

$$\hat{\sigma}(q\bar{q}\to h) = \frac{4\pi^2 m_h}{9\hat{s}}\Gamma_{h\to q\bar{q}}\,\delta(\hat{s}-m_h^2). \tag{27}$$

Naïvely, one would expect $\hat{\sigma}(q\bar{q}\to h)$ for the heavier quarks to be larger than the lighter ones as $\Gamma_{h\to q\bar{q}}$ is proportional to the square of $y_q^{\rm eff}$ (which increases linearly with m_q). However, there is a trade-off between m_q and the PDFs as the heavier quarks PDFs are suppressed than their lighter counterparts. We compute $\sigma(q\bar{q}\to h)$ at the 14 TeV LHC using the NNPDF2.3QED LO [62] PDF. Similarly, we use the NNLO+NNLL QCD prediction for the 14 TeV LHC which leads $\sigma(gg\to h)_{\rm SM}\simeq 49.47$ pb [63]. We use these results to compute $\mu_{\rm F}$. We show $\mu_{\rm F}$ as a function of M_{S_1} in Fig. 4(a) assuming $g^2 y_\nu = 1$ for all the generations and $\lambda = 1$. For this plot we set $M_{\nu_R} = 1$ TeV. However, since the gluon fusion cross section is much larger than the quark fusion ones, $\mu_{\rm F}$ is largely insensitive to M_{ν_R}.

To get an idea of the contributions of the different modes to $\mu_{\rm F}$ we define the following two ratios,

$$R_h(ii\to h) = \frac{\sigma(ii\to h)}{\sigma(gg\to h)_{\rm SM}} \quad \text{(full model)}, \tag{28}$$

$$R_h^{\rm BSM}(ii\to h) = \frac{\sigma(ii\to h)_{\rm BSM}}{\sigma(gg\to h)_{\rm SM}} \quad \text{(BSM only)}. \tag{29}$$

The difference between these two ratios lies in the interference between the SM and BSM contributions. We show these ratios in Figs. 4(b) and 4(c). We find, that even after the PDF suppression, $R_h(b\bar{b}\to h) > R_h(s\bar{s}\to h) > R_h(d\bar{d}\to h)$. On the other hand if we take $R_h^{\rm BSM}$, the hierarchy is reversed. This can be understood from the fact that the loop contribution δy is equal for all the three quarks and hence the PDF suppression makes $R_h^{\rm BSM}(b\bar{b}\to h) < R_h^{\rm BSM}(s\bar{s}\to h) < R_h^{\rm BSM}(d\bar{d}\to h)$. Of course, because of the large gluon PDF, $\sigma(gg\to h)$ is larger than any quark fusion cross section.

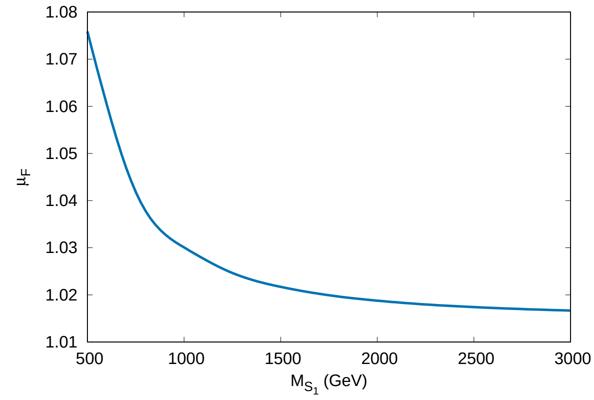

(a)

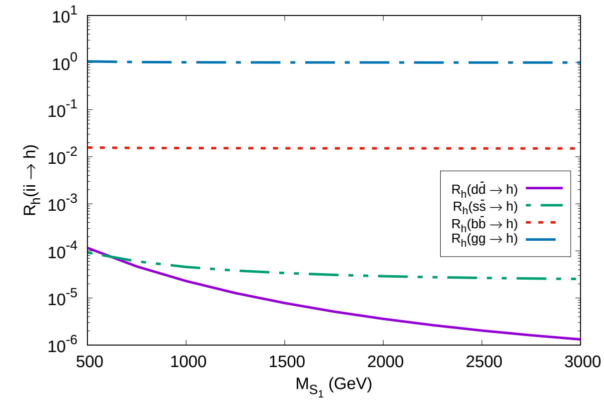

(b)

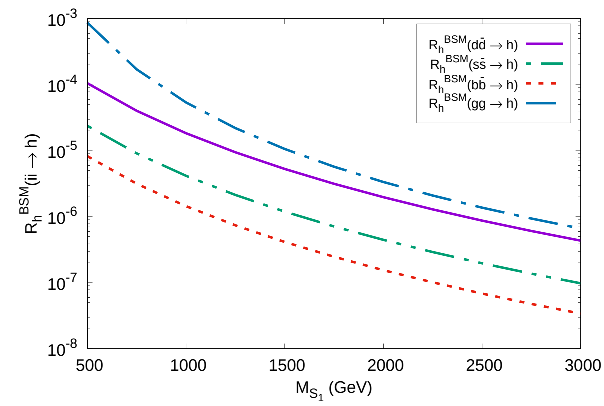

(c)

FIG. 4. (a) The normalized production cross-section of h_{125} as a function of M_{S_1} for $M_{\nu_R} = 1$ TeV. Here also we take $g^2 y_\nu = 1$ for all the generations and $\lambda = 1$. (b) Relative production factor ($\rm R_h$) (defined in the text) for SM+LQ scenario as a function of M_{S_1} for $M_{\nu_R} = 1$ TeV. (c) Relative production factor ($\rm R_h^{BSM}$) as a function of M_{S_1} for $M_{\nu_R} = 1$ TeV when the $hq\bar{q}$ (hgg) coupling at the leading order in SM is assumed to be zero.

IV. LIMITS ON PARAMETERS

Any increase in either the productions and/or the decays of h_{125} would be constrained by the existing measurements [3] (also see [64] for future projections). However we see from Figs. 3 and 4, that the parameters we consider, i.e., $g_i^2 =$

$y_i^{LL} y_i^{\overline{RR}} = 1$, $y_i^{RR} = 0$, $\lambda = 1$, $y_\nu = 1$ and TeV-scale M_{S_1}, M_{ν_R} for all the three generations are quite consistent with the present and future h_{125} limits.

Concerning the bounds on S_1, we see that in the parameter region of our interest, LQ S_1 can decay to all the SM fermions. According to Eq. (4) and Eq. (7), a heavy S_1 would have six decay modes for $M_{S_1} \leq M_{\nu_R}$:

$$S_1 \to \{ue, c\mu, t\tau, d\nu, s\nu, b\nu\}, \tag{30}$$

with roughly equal BR ($\sim 1/6$) in each mode (if we ignore the differences among the masses of the decay products in different modes). The LHC has put exclusion bounds on scalar leptoquarks in the light-leptons+jets ($\ell\ell jj/\ell\nu jj$) [65–67] and $bb\nu\nu/tt\tau\tau$ [68–70] channels (also see [71, 72]). The strongest exclusion limit (~ 1.5 TeV) comes from the $\ell\ell jj$ channel for 100% BR in the $S_1 \to \ell j$ decay. These searches are for pair production of scalar leptoquarks, where the observable signal cross sections are proportional to the square of the BR involved. Hence, in our case, the limit on S_1 would get much weaker. A conservative estimation indicates that the limit goes below a TeV when the BR decreases to about $1/6$. Also, pair productions of leptoquarks are QCD driven and thus cannot be used to put limits on the fermion couplings. The CMS collaboration has performed a search with the 8 TeV data for single production of scalar leptoquarks that excludes up to 1.75 TeV for order one coupling to the first generation [73]. However, even that limit comes down below one TeV once we account for the reduction in the BR. However, a recast of CMS 8 TeV data for the first generation ($eejj/e\nu jj$) indicates that for order one $g_{(L/R)}$, $M_{S_1} \gtrsim 1.1$ TeV [74].[2] To be on the conservative side, we may use $M_{S_1} \gtrsim 1.5$ TeV as a mass limit for S_1 with $g^2 y_\nu = 1$ for all generations.

If, however, $M_{S_1} > M_{\nu_R}$, the LQ can decay to three more final states with right-handed neutrinos. So, we would expect further reduction of the limits on S_1 [31]. Moreover, specifically for the first generation fermions, the choice of g_L and g_R are restricted further. The Atomic parity violation measurements in Cs^{133} [75] put a strong constraint on them. Typically, all existing constraints may be satisfied easily for $M_{S_1} \gtrsim 2$ TeV and $g^2 \approx 1$ with $g_L = g_R$.

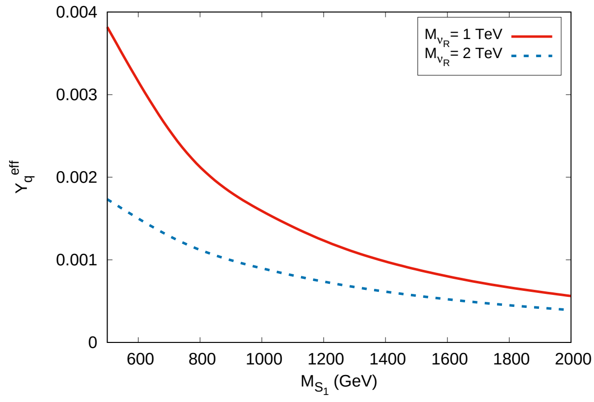

FIG. 6. Variation of $\phi q\bar{q}$ coupling as a function of M_{S_1} for $M_{\nu_R} = 1$ TeV and 2 TeV, $g^2 y_\nu = 1$, $\lambda' = 2$ TeV and $M_\phi = 500$ GeV.

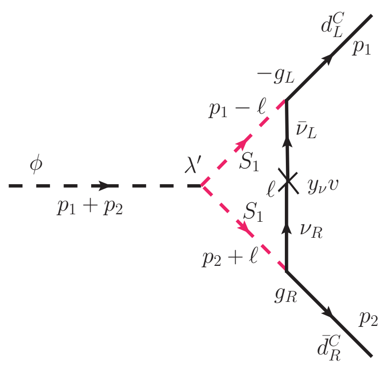

FIG. 5. The singlet scalar, ϕ decaying to down-type quarks.

V. THE SINGLET HIGGS ϕ

Unlike the case of h_{125}, the parameters of the singlet scalar defined in Eq. (4) are largely unconstrained. To probe a heavy BSM scalar, generally, its decays to fermion pairs like $\tau\tau$ or the massive gauge bosons are assumed to be promising. But, for a singlet scalar, these decay modes lose importance. Also, most of the BSM singlet scalar searches rely on the mixing among the singlet state with the doublet one(s), either h_{125} or other BSM heavy Higgs states. In our model, in contrast, ϕ's can be produced from and decay to a pair of gluons or quarks via the loop of S_1 and neutrinos without relying on the mixing of ϕ with the doublet Higgs in general. Hence, its phenomenology at the hadron collider would be different than what is generally considered in the literature.

A. Effective Coupling

We first calculate the effective couplings of ϕ to the light quarks, as we did for h_{125}. The $\phi q\bar{q}$ effective coupling, $Y_q^{\rm eff}$ (where q is any down-type quark) would receive contribution from diagrams like the one shown in Fig. 5, which is similar to the one shown in Fig. 1(d). Because of the singlet nature of ϕ, the tree level $\phi \bar{\nu}_L \nu_R$ coupling does not exist and so, in this case, there is no diagram like the one shown in Fig. 1(c). Proceeding like before we get,

$$Y_q^{\rm eff} = \frac{g^2 \lambda' y_\nu v}{16\pi^2} \int_0^1 dx \int_0^{1-x} dy \left(\frac{1}{D_\phi}\right),$$

where,

$$D_\phi(x,y) = M_{\nu_R}^2 + (x+y)(M_{S_1}^2 - M_{\nu_R}^2) - xy M_\phi^2. \tag{31}$$

Written in terms of PV integrals this becomes,

$$Y_q^{\rm eff} = -\frac{g^2 \lambda' y_\nu v}{16\pi^2} C_0(0,0,M_\phi^2, M_{S_1}^2, M_{\nu_R}^2, M_{S_1}^2). \tag{32}$$

[2] Recasting limits from the single production searches is trickier than the pair production case because here the production processes also depend on the unknown couplings. Even though the parton level cross section scale easily with these couplings, one cannot account for the PDF variation for different quarks in such a simple manner. Since we are interested in a conservative limit, we have ignored the PDF variation to obtain this number.

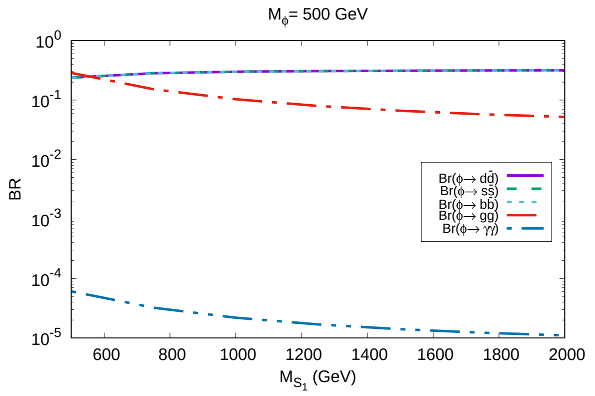

(a)

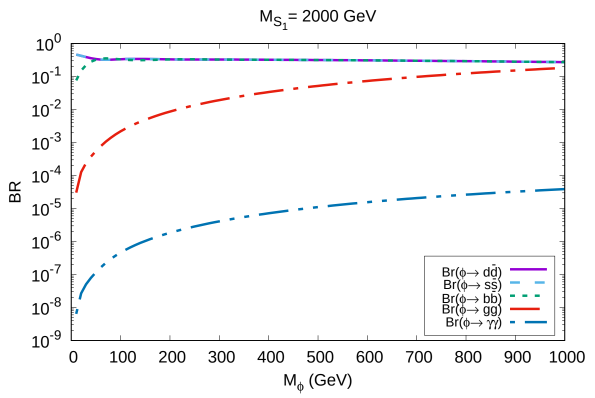

(b)

FIG. 7. Variation of Br $(\phi \to q\bar{q})$, Br $(\phi \to gg)$ and Br $(\phi \to \gamma\gamma)$ as a function of M_{S_1}(a) and M_ϕ(b) for $g^2 y_\nu = 1$ and $M_{\nu_R} = 1$ TeV. The ratios are independent of λ'. We set it at 2 TeV to compute the partial decay widths of ϕ.

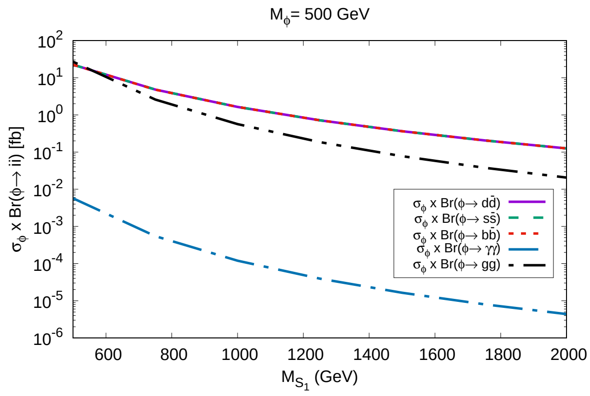

(a)

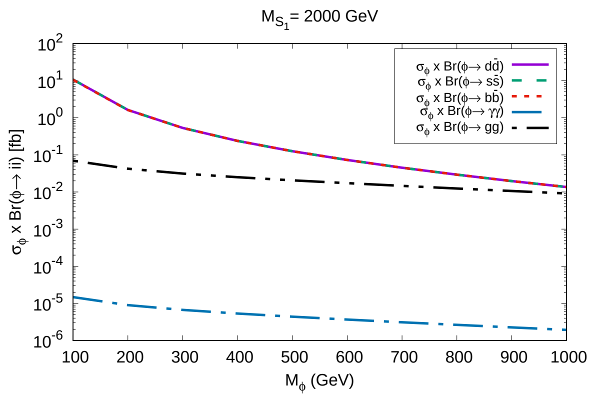

(b)

FIG. 8. Variation of the production cross section of ϕ times the branching ratios as functions of (a) M_{S_1} and (b) M_ϕ for $g^2 y_\nu = 1$, $\lambda' = 2$ TeV and $M_{\nu_R} = 1$ TeV at the 14 TeV LHC.

We present our results in Fig. 6, which shows the variation of $Y_q^{\rm eff}$ as a function of M_{S_1} for two values of M_{ν_R} and $M_\phi = 500$ GeV. Here, λ' is a dimensionful parameter [see Eq. (4)] that can be taken to be of the order of the largest mass in the model spectrum. The coupling, $Y_q^{\rm eff}$ decreases as M_{S_1} increases. Since ϕ has only loop-level interaction with the SM quarks, the effective coupling is same for all the three generations of down-type quarks for the same value of $g^2 y_\nu$.

B. Branching Ratios and Cross Sections

The expressions for the partial decay widths and production cross section of ϕ are essentially identical as the ones for h_{125} if we replace $y_q^{\rm eff} \to Y_q^{\rm eff}$ and $m_h \to M_\phi$. Thus, the expressions for the partial decay widths would look like,

$$\Gamma_{\phi\to q\bar{q}} = \frac{3|Y_q^{\rm eff}|^2}{8\pi M_\phi^2}\left(M_\phi^2 - 4m_q^2\right)^{3/2} \approx \frac{3}{8\pi}|Y_q^{\rm eff}|^2 M_\phi, \tag{33}$$

$$\Gamma_{\phi\to gg} = \frac{G_{\rm F}\alpha_S^2 M_\phi^3}{64\sqrt{2}\pi^3}\left|\frac{\lambda' v}{2M_{S_1}^2}\mathscr{A}_0\left(\frac{M_\phi^2}{4M_{S_1}^2}\right)\right|^2, \tag{34}$$

$$\Gamma_{\phi\to\gamma\gamma} = \frac{G_{\rm F}\alpha_{\rm em}^2 M_\phi^3}{128\sqrt{2}\pi^3}\left|\frac{\lambda' v}{6M_{S_1}^2}\mathscr{A}_0\left(\frac{M_\phi^2}{4M_{S_1}^2}\right)\right|^2. \tag{35}$$

The Feynman diagrams for $\phi \to \gamma\gamma$ process will be similar to those in Figs. 1(a) and 1(b) with the gluons replaced by two photons and the α_s coupling is substituted with the $\alpha_{\rm em}$ coupling. As earlier, we can now express the cross sections in these modes in terms of the partial widths. In the gg channel,

$$\hat{\sigma}(gg \to \phi) = \frac{\pi^2 M_\phi}{8\hat{s}}\Gamma_{h\to gg}\delta(\hat{s} - M_\phi^2), \tag{36}$$

and in the $q\bar{q}$ channel,

$$\hat{\sigma}(q\bar{q} \to \phi) = \frac{4\pi^2 M_\phi}{9\hat{s}}\Gamma_{\phi\to q\bar{q}}\delta(\hat{s} - M_\phi^2). \tag{37}$$

The total width for ϕ can be expressed as,

$$\Gamma_\phi = \left(\sum_{q=d,s,b}\Gamma_{\phi\to q\bar{q}} + \Gamma_{\phi\to gg} + \Gamma_{\phi\to\gamma\gamma}\right). \tag{38}$$

We now present our numerical results. We begin with Fig. 7 where we show the variation of BRs of different decay modes of ϕ. For most part, the plots for the quarks overlap as $\Gamma_{\phi\to q\bar{q}}$ is essentially independent of m$_q$ [see Eq. (33)]. Here, without any singlet-doublet mixing, ϕ can only decay to down-type

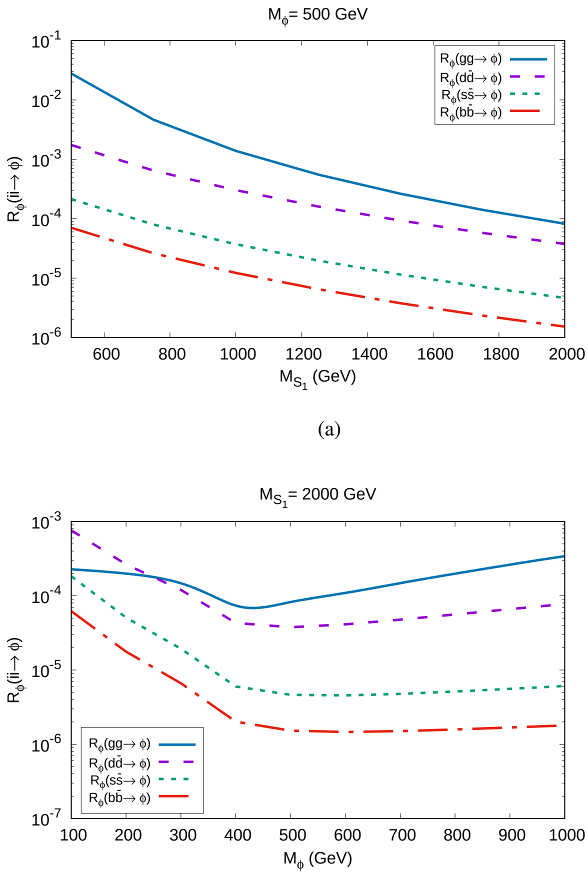

(a)

(b)

FIG. 9. Variation of $R_\phi(ii \to \phi)$ [Eq. (40)] with (a) M_{S_1} and (b) M_ϕ for $g^2 y_\nu = 1$, $\lambda' = 2$ TeV and $M_{\nu_R} = 1$ TeV.

quarks, gluon or photon pairs. As a result, when M_{S_1} increases, $\mathrm{Br}(\phi \to gg/\gamma\gamma)$ decreases and $\mathrm{Br}(\phi \to q\bar{q})$ goes up if M_{ν_R} is held fixed. We see that for a 2 TeV S_1, $\phi \to q\bar{q}$ is the dominant decay mode for $g^2 y_\nu = 1$, $M_{\nu_R} = 1$ TeV (the BRs are independent of λ').

In Figs. 8(a) and 8(b), we plot the scattering cross sections of ϕ in different decay modes at the 14 TeV LHC, considering both the gluon and quark fusion processes. We show the production cross section times the branching ratio for all the modes, against M_{S_1} and M_ϕ. Note that in the parameter space we consider, we find $\Gamma_\phi \ll M_\phi$ which makes the narrow width approximation used in our computation as a valid one. Here, we use the same set of PDFs as in the h_{125} case. To have some intuition about the strengths of different production channels, we scale the cross sections by $\sigma(gg \to h_{M_\phi})$ where h_{M_ϕ} represents a BSM Higgs whose couplings with the SM particles are the same as those of h_{125}. Its production cross section in the gluon fusion mode can be computed from Eq. (26) after taking $M_{S_1} \to \infty$ in Eq. (19) as,

$$\hat{\sigma}(gg \to h_{M_\phi}) \simeq \frac{G_{\mathrm{F}} \alpha_S^2 M_\phi^4}{512\sqrt{2}\pi \hat{s}} \left| \mathscr{A}_{1/2}\left(\frac{M_\phi^2}{4m_t^2}\right) \right|^2 \delta(\hat{s} - M_\phi^2). \quad (39)$$

Then we define the scaled cross sections as,

$$R_\phi(ii \to \phi) = \frac{\sigma(ii \to \phi)}{\sigma(gg \to h_{M_\phi})}. \quad (40)$$

In Figs. 9(a) and 9(b), we show the variation of R_ϕ with M_{S_1} and M_ϕ. Recall that, a SM singlet ϕ cannot be produced at the tree level. The leading order contribution to $\sigma(ii \to \phi)$ starts at the one-loop level. In Fig. 9(b), we observe a cross-over where the qqF becomes the dominant process over the ggF, i.e., $\sigma(q\bar{q} \to \phi) > \sigma(gg \to \phi)$ for a fixed value of LQ mass ($= 2$ TeV). This is not a generic pattern and can be understood from Eqs. (33) and (34) by varying a few of the free parameters. For example, a relatively large value of LQ mass ($M_{S_1} \geq 2$ TeV), one may obtain $\Gamma_{\phi \to gg} \leq \Gamma_{\phi \to q\bar{q}}$ when ϕ is not large i.e., $M_\phi \lesssim 250$ GeV. In this case, quark fusion process would have the leading contributions. If one increases M_{S_1} further, $\Gamma_{\phi \to gg}$ would decrease more rapidly than $\Gamma_{\phi \to q\bar{q}}$ with M_ϕ ensuring the $q\bar{q} \to \phi$ process remains the dominant one for a bigger range of M_ϕ. For example, if one sets $M_{S_1} \sim 3$ TeV, we find that quark fusion becomes dominant for $M_\phi \lesssim 350$ GeV. However, the relative contributions are insensitive to the value of λ' chosen.

C. Prospects at the LHC

It is clear that the scalar ϕ in our model would offer some novel and interesting phenomenology at the LHC. However, a detailed analysis is beyond the scope of this paper. Instead we just make a few comments on its prospects.

It may be possible to put a bound on $\sigma_\phi(M_\phi)$ from the dijet resonance searches. For example, the one performed by the CMS collaboration at the 13 TeV LHC [76] indicates that $\sigma_\phi \times \mathrm{Br}(\phi \to gg)$ has to be less than about 1 pb for $M_\phi = 1$ TeV and about 20 pb for $M_\phi = 600$ GeV. Similarly, in the quark mode, $\sigma_\phi \times \mathrm{Br}(\phi \to d\bar{d} + s\bar{s} + b\bar{b})$ is less than about 1 pb for $M_\phi = 1$ TeV and about 5 pb for $M_\phi = 600$ GeV. Fig. 8(b) (which is obtained for the 14 TeV LHC) indicates our choice of parameters easily satisfies this limit. Future searches in this channel would put stronger bounds on σ_ϕ and/or M_ϕ. The LHC has also searched for such a state in the $\gamma\gamma$ final states, though, the present bound from this channel is weaker [77] than the dijet one. In our model, this channel is not at all promising as can be seen from Figs. 8 and 9. Even the HL-LHC might not be able to probe the singlet state in the $\gamma\gamma$ mode.

VI. CONCLUSION

In this paper, we have considered a simple extension to the SM, in which we have a scalar LQ (S_1) with electromagnetic charge $1/3$ and heavy right chiral neutrinos. While the presence of both BSM particles may have their origin at grand unified framework, we simply consider their interactions at the TeV scale. The motivation for considering such an extension comes from the fact that it can accommodate enhanced Yukawa couplings of the down-type quarks that are still allowed by the current experimental searches.

We have shown that the LQ and the right chiral neutrinos can enhance the production cross-section of the SM-like Higgs through a triangle loop. We have calculated the one loop contributions to the Yukawa couplings of the down-type quarks. We have found the enhancements (which we have parametrized by the usual $\kappa_{d,s,b}$) to be within the allowed ranges for order one new couplings and TeV scale new particles. They may be probed at the HL-LHC. We have then further extended our analysis to include a SM-singlet scalar ϕ in the model with a dimension one coupling with S_1 but no tree-level mixing with the SM-like Higgs. We have found that for similar choice of parameters, the gluon fusion (through a LQ in the loop) and the quark fusion (mediated by a LQ and neutrinos in a loop) processes can lead to a significant cross section to produce ϕ at the LHC. They also enhance the decay width of the singlet. Interestingly, we find that for a light ϕ, the quark fusion can become more important than the gluon fusion process as long as the mass of the LQ remains high ($\sim$ TeV). In both cases, precise measurements of branching fractions or partial widths of the 125 GeV SM-like Higgs or the singlet scalar i.e., $h_{125}, \phi \to d\bar{d}, s\bar{s}, b\bar{b}$ would be crucial to test or constrain the model at the high luminosity run of the LHC.

ACKNOWLEDGMENTS

Our computations were supported in part by SAMKHYA: the High Performance Computing Facility provided by the Institute of Physics (IoP), Bhubaneswar. A. B. and S. M. acknowledge support from the Science and Engineering Research Board (SERB), DST, India under Grant No. ECR/2017/000517. We thank P. Agrawal for a helpful discussion. S. M. also acknowledges the local hospitality at IoP, Bhubaneswar during the meeting, IMHEP-19 where this work was initiated.

[1] ATLAS collaboration, G. Aad et al., *Observation of a new particle in the search for the Standard Model Higgs boson with the ATLAS detector at the LHC*, Phys. Lett. **B716** (2012) 1–29, [1207.7214].

[2] CMS collaboration, S. Chatrchyan et al., *Observation of a New Boson at a Mass of 125 GeV with the CMS Experiment at the LHC*, Phys. Lett. **B716** (2012) 30–61, [1207.7235].

[3] ATLAS collaboration, G. Aad et al., *Combined measurements of Higgs boson production and decay using up to 80 fb^{-1} of proton-proton collision data at $\sqrt{s}$ = 13 TeV collected with the ATLAS experiment*, 1909.02845.

[4] CMS collaboration, V. Khachatryan et al., *Search for a standard model-like Higgs boson in the $\mu^+\mu^-$ and e^+e^- decay channels at the LHC*, Phys. Lett. **B744** (2015) 184–207, [1410.6679].

[5] G. Perez, Y. Soreq, E. Stamou and K. Tobioka, *Constraining the charm Yukawa and Higgs-quark coupling universality*, Phys. Rev. **D92** (2015) 033016, [1503.00290].

[6] A. L. Kagan, G. Perez, F. Petriello, Y. Soreq, S. Stoynev and J. Zupan, *Exclusive Window onto Higgs Yukawa Couplings*, Phys. Rev. Lett. **114** (2015) 101802, [1406.1722].

[7] L. Alasfar, R. Corral Lopez and R. Gröber, *Probing Higgs couplings to light quarks via Higgs pair production*, JHEP **11** (2019) 088, [1909.05279].

[8] J. de Blas et al., *Higgs Boson Studies at Future Particle Colliders*, JHEP **01** (2020) 139, [1905.03764].

[9] S. Bar-Shalom and A. Soni, *Universally enhanced light-quarks Yukawa couplings paradigm*, Phys. Rev. **D98** (2018) 055001, [1804.02400].

[10] J. Cohen, S. Bar-Shalom, G. Eilam and A. Soni, *R-Parity Violating Supersymmetry and the 125 GeV Higgs signals*, 1906.04743.

[11] J. C. Pati and A. Salam, *Unified lepton-hadron symmetry and a gauge theory of the basic interactions*, Phys. Rev. D **8** (1973) 1240 – 1251.

[12] H. Georgi and S. L. Glashow, *Unity of all elementary-particle forces*, Phys. Rev. Lett. **32** (1974) 438–441.

[13] H. Georgi, *The state of the art—gauge theories*, AIP Conference Proceedings **23** (1975) 575–582.

[14] I. Doršner, S. Fajfer, A. Greljo, J. F. Kamenik and N. Košnik, *Physics of leptoquarks in precision experiments and at particle colliders*, Phys. Rept. **641** (2016) 1–68, [1603.04993].

[15] S. Fajfer and N. Košnik, *Vector leptoquark resolution of R_K and $R_{D^{(*)}}$ puzzles*, Phys. Lett. **B755** (2016) 270–274, [1511.06024].

[16] R. Barbieri, G. Isidori, A. Pattori and F. Senia, *Anomalies in B-decays and $U(2)$ flavour symmetry*, Eur. Phys. J. **C76** (2016) 67, [1512.01560].

[17] I. Doršner, S. Fajfer, N. Košnik and I. Nišandžić, *Minimally flavored colored scalar in $\bar{B} \to D^{(*)}\tau\bar{\nu}$ and the mass matrices constraints*, JHEP **11** (2013) 084, [1306.6493].

[18] B. Gripaios, M. Nardecchia and S. A. Renner, *Composite leptoquarks and anomalies in B-meson decays*, JHEP **05** (2015) 006, [1412.1791].

[19] D. Bečirević, S. Fajfer and N. Košnik, *Lepton flavor nonuniversality in $b \to s\ell^+\ell^-$ processes*, Phys. Rev. **D92** (2015) 014016, [1503.09024].

[20] D. Bečirević, S. Fajfer, N. Košnik and O. Sumensari, *Leptoquark model to explain the B-physics anomalies, R_K and R_D*, Phys. Rev. **D94** (2016) 115021, [1608.08501].

[21] J. M. Cline, *B decay anomalies and dark matter from vectorlike confinement*, Phys. Rev. **D97** (2018) 015013, [1710.02140].

[22] L. Di Luzio and M. Nardecchia, *What is the scale of new physics behind the B-flavour anomalies?*, Eur. Phys. J. **C77** (2017) 536, [1706.01868].

[23] U. Aydemir, T. Mandal and S. Mitra, *Addressing the $\mathbf{R}_{D^{(*)}}$ anomalies with an $\mathbf{S}_1$ leptoquark from $\mathbf{SO(10)}$ grand unification*, Phys. Rev. **D101** (2020) 015011, [1902.08108].

[24] T. Mandal, S. Mitra and S. Raz, *$R_{D^{(*)}}$ motivated $\mathscr{S}_1$ leptoquark scenarios: Impact of interference on the exclusion limits from LHC data*, Phys. Rev. **D99** (2019) 055028, [1811.03561].

[25] K. Cheung, W. Y. Keung and P. Y. Tseng, *Leptoquark induced rare decay amplitudes $h \to \tau^{\mp}\mu^{\pm}$ and $\tau \to \mu\gamma$*, Phys. Rev. D **93** (2016) 015010.

[26] R. Mandal, *Fermionic dark matter in leptoquark portal*, Eur. Phys. J. **C78** (2018) 726, [1808.07844].

[27] S.-M. Choi, Y.-J. Kang, H. M. Lee and T.-G. Ro, *Lepto-Quark Portal Dark Matter*, JHEP **10** (2018) 104, [1807.06547].

[28] A. Djouadi, T. Köhler, M. Spira and J. Tutas, *(eb), (et) type leptoquarks atep colliders*, Zeitschrift für Physik C Particles and Fields **46** (Dec, 1990) 679–685.

[29] K.-m. Cheung, *Muon anomalous magnetic moment and leptoquark solutions*, Phys. Rev. **D64** (2001) 033001, [hep-ph/0102238].

[30] I. Doršner, S. Fajfer and O. Sumensari, *Muon $g-2$ and scalar leptoquark mixing*, 1910.03877.

[31] D. Das, K. Ghosh, M. Mitra and S. Mondal, *Probing sterile neutrinos in the framework of inverse seesaw mechanism through leptoquark productions*, Phys. Rev. **D97** (2018) 015024, [1708.06206].

[32] T. Mandal, S. Mitra and S. Seth, *Pair Production of Scalar Leptoquarks at the LHC to NLO Parton Shower Accuracy*,

Phys. Rev. **D93** (2016) 035018, [1506.07369].
[33] I. Doršner, S. Fajfer, D. A. Faroughy and N. Košnik, *The role of the S_3 GUT leptoquark in flavor universality and collider searches*, 1706.07779. [JHEP10,188(2017)].
[34] G. Hiller, D. Loose and I. Nišandžić, *Flavorful leptoquarks at hadron colliders*, *Phys. Rev.* **D97** (2018) 075004, [1801.09399].
[35] A. Biswas, A. Shaw and A. K. Swain, *Collider signature of V_2 Leptoquark with $b \to s$ flavour observables*, *LHEP* **2** (2019) 126, [1811.08887].
[36] T. Faber, Y. Liu, W. Porod, M. Hudec, M. Malinský, F. Staub et al., *Collider phenomenology of a unified leptoquark model*, 1812.07592.
[37] K. Chandak, T. Mandal and S. Mitra, *Hunting for scalar leptoquarks with boosted tops and light leptons*, *Phys. Rev.* **D100** (2019) 075019, [1907.11194].
[38] R. Padhan, S. Mandal, M. Mitra and N. Sinha, *Signatures of $\tilde{R}_2$ class of Leptoquarks at the upcoming ep colliders*, 1912.07236.
[39] B. C. Allanach, T. Corbett and M. Madigan, *Sensitivity of Future Hadron Colliders to Leptoquark Pair Production in the Di-Muon Di-Jets Channel*, 1911.04455.
[40] R. N. Mohapatra, *Mechanism for understanding small neutrino mass in superstring theories*, *Phys. Rev. Lett.* **56** (Feb, 1986) 561–563.
[41] S. Nandi and U. Sarkar, *Solution to the neutrino-mass problem in superstring e_6 theory*, *Phys. Rev. Lett.* **56** (Feb, 1986) 564–567.
[42] R. N. Mohapatra and J. W. F. Valle, *Neutrino mass and baryon-number nonconservation in superstring models*, *Phys. Rev. D* **34** (Sep, 1986) 1642–1645.
[43] F. Deppisch and J. W. F. Valle, *Enhanced lepton flavor violation in the supersymmetric inverse seesaw model*, *Phys. Rev.* **D72** (2005) 036001, [hep-ph/0406040].
[44] A. Abada, D. Das and C. Weiland, *Enhanced Higgs Mediated Lepton Flavour Violating Processes in the Supersymmetric Inverse Seesaw Model*, *JHEP* **03** (2012) 100, [1111.5836].
[45] A. Abada, D. Das, A. Vicente and C. Weiland, *Enhancing lepton flavour violation in the supersymmetric inverse seesaw beyond the dipole contribution*, *JHEP* **09** (2012) 015, [1206.6497].
[46] S. Mondal, S. Biswas, P. Ghosh and S. Roy, *Exploring novel correlations in trilepton channels at the LHC for the minimal supersymmetric inverse seesaw model*, *JHEP* **05** (2012) 134, [1201.1556].
[47] A. Abada, M. E. Krauss, W. Porod, F. Staub, A. Vicente and C. Weiland, *Lepton flavor violation in low-scale seesaw models: SUSY and non-SUSY contributions*, *JHEP* **11** (2014) 048, [1408.0138].
[48] E. Arganda, M. J. Herrero, X. Marcano and C. Weiland, *Imprints of massive inverse seesaw model neutrinos in lepton flavor violating Higgs boson decays*, *Phys. Rev.* **D91** (2015) 015001, [1405.4300].
[49] E. Arganda, M. J. Herrero, X. Marcano and C. Weiland, *Enhancement of the lepton flavor violating Higgs boson decay rates from SUSY loops in the inverse seesaw model*, *Phys. Rev.* **D93** (2016) 055010, [1508.04623].
[50] P. Agrawal and U. Mahanta, *Leptoquark contribution to the Higgs boson production at the CERN LHC collider*, *Phys. Rev.* **D61** (2000) 077701, [hep-ph/9911497].
[51] U. Ellwanger, C. Hugonie and A. M. Teixeira, *The Next-to-Minimal Supersymmetric Standard Model*, *Phys. Rept.* **496** (2010) 1–77, [0910.1785].
[52] D. Das, *Dominant production of heavier Higgs bosons through vector boson fusion in the NMSSM*, *Phys. Rev.* **D99** (2019) 095035, [1804.06630].
[53] R. Mandal and A. Pich, *Constraints on scalar leptoquarks from lepton and kaon physics*, *JHEP* **12** (2019) 089, [1908.11155].
[54] E. Arganda, M. J. Herrero, X. Marcano, R. Morales and A. Szynkman, *Effective lepton flavor violating $H\ell_i\ell_j$ vertex from right-handed neutrinos within the mass insertion approximation*, *Phys. Rev.* **D95** (2017) 095029, [1612.09290].
[55] G. Passarino and M. J. G. Veltman, *One Loop Corrections for e+ e- Annihilation Into mu+ mu- in the Weinberg Model*, *Nucl. Phys.* **B160** (1979) 151–207.
[56] V. Shtabovenko, R. Mertig and F. Orellana, *New Developments in FeynCalc 9.0*, *Comput. Phys. Commun.* **207** (2016) 432–444, [1601.01167].
[57] T. Hahn and M. Perez-Victoria, *Automatized one loop calculations in four-dimensions and D-dimensions*, *Comput. Phys. Commun.* **118** (1999) 153–165, [hep-ph/9807565].
[58] PARTICLE DATA GROUP collaboration, M. Tanabashi et al., *Review of particle physics*, *Phys. Rev. D* **98** (2018) 030001.
[59] A. Djouadi, *The Anatomy of electro-weak symmetry breaking. II. The Higgs bosons in the minimal supersymmetric model*, *Phys. Rept.* **459** (2008) 1–241, [hep-ph/0503173].
[60] J. F. Gunion and H. E. Haber, *Higgs Bosons in Supersymmetric Models. 2. Implications for Phenomenology*, *Nucl. Phys.* **B278** (1986) 449. [Erratum: Nucl. Phys.B402,569(1993)].
[61] W.-F. Chang, J. N. Ng and J. M. S. Wu, *Constraints on New Scalars from the LHC 125 GeV Higgs Signal*, *Phys. Rev.* **D86** (2012) 033003, [1206.5047].
[62] NNPDF collaboration, R. D. Ball, V. Bertone, S. Carrazza, L. Del Debbio, S. Forte, A. Guffanti et al., *Parton distributions with QED corrections*, *Nucl. Phys.* **B877** (2013) 290–320, [1308.0598].
[63] https://twiki.cern.ch/twiki/bin/view/LHCPhysics/CERNYello
[64] M. Cepeda et al., *Report from Working Group 2*, *CERN Yellow Rep. Monogr.* **7** (2019) 221–584, [1902.00134].
[65] ATLAS collaboration, M. Aaboud et al., *Searches for scalar leptoquarks and differential cross-section measurements in dilepton-dijet events in proton-proton collisions at a centre-of-mass energy of $\sqrt{s}$ = 13 TeV with the ATLAS experiment*, *Eur. Phys. J.* **C79** (2019) 733, [1902.00377].
[66] CMS collaboration, A. M. Sirunyan et al., *Search for pair production of first-generation scalar leptoquarks at $\sqrt{s} = 13$ TeV*, *Phys. Rev.* **D99** (2019) 052002, [1811.01197].
[67] CMS collaboration, A. M. Sirunyan et al., *Search for pair production of second-generation leptoquarks at $\sqrt{s} = 13$ TeV*, *Phys. Rev.* **D99** (2019) 032014, [1808.05082].
[68] CMS collaboration, A. M. Sirunyan et al., *Constraints on models of scalar and vector leptoquarks decaying to a quark and a neutrino at $\sqrt{s} = 13$ TeV*, *Phys. Rev.* **D98** (2018) 032005, [1805.10228].
[69] CMS collaboration, A. M. Sirunyan et al., *Search for leptoquarks coupled to third-generation quarks in proton-proton collisions at $\sqrt{s} = 13$ TeV*, *Phys. Rev. Lett.* **121** (2018) 241802, [1809.05558].
[70] ATLAS collaboration, M. Aaboud et al., *Searches for third-generation scalar leptoquarks in $\sqrt{s}$ = 13 TeV pp collisions with the ATLAS detector*, *JHEP* **06** (2019) 144, [1902.08103].
[71] CMS collaboration, Y. Takahashi, *Leptoquark searches in CMS*, in *Proceedings, 53rd Rencontres de Moriond on Electroweak Interactions and Unified Theories (Moriond EW 2018): La Thuile, Italy, March 10-17, 2018*, pp. 65–70, 2018. 1901.03570.
[72] ATLAS collaboration, V. W. S. Wong, *Searching for leptoquarks with the ATLAS detector*, in *17th Conference on Flavor Physics and CP Violation (FPCP 2019) Victoria, BC, Canada, May 6-10, 2019*, 2019. 1906.08983.
[73] CMS collaboration, V. Khachatryan et al., *Search for single production of scalar leptoquarks in proton-proton collisions at*

$\sqrt{s} = 8$ *TeV*, *Phys. Rev.* **D93** (2016) 032005, [1509.03750]. [Erratum: Phys. Rev.D95,no.3,039906(2017)].

[74] T. Mandal, S. Mitra and S. Seth, *Single Productions of Colored Particles at the LHC: An Example with Scalar Leptoquarks*, *JHEP* **07** (2015) 028, [1503.04689].

[75] P. Langacker, *Parity violation in muonic atoms and cesium*, *Physics Letters B* **256** (1991) 277 – 283.

[76] CMS collaboration, A. M. Sirunyan et al., *Search for dijet resonances in proton–proton collisions at $\sqrt{s}$ = 13 TeV and constraints on dark matter and other models*, *Phys. Lett.* **B769** (2017) 520–542, [1611.03568]. [Erratum: Phys. Lett.B772,882(2017)].

[77] ATLAS collaboration, M. Aaboud et al., *Search for new phenomena in high-mass diphoton final states using 37 fb^{-1} of proton–proton collisions collected at $\sqrt{s} = 13$ TeV with the ATLAS detector*, *Phys. Lett.* **B775** (2017) 105–125, [1707.04147].